

Influences of Marangoni convection and variable magnetic field on hybrid nanofluid thin-film flow past a stretching surface

Noor Wali Khan, Arshad Khan, Muhammad Usman, Taza Gul, Abir Mouldi, and Ameni Brahmia

Citation: Chin. Phys. B, 2022, 31 (**6**): 064403. DOI: 10.1088/1674-1056/ac3a5d
Journal homepage: http://cpb.iphy.ac.cn; http://iopscience.iop.org/cpb

What follows is a list of articles you may be interested in

Investigation of hypersonic flows through a cavity with sweepback angle in near space using the DSMC method

Guangming Guo(郭广明), Hao Chen(陈浩), Lin Zhu(朱林), and Yixiang Bian(边义祥)
Chin. Phys. B, 2021, 30 (**7**): 074701. DOI: 10.1088/1674-1056/abf7ad

Flow characteristics of supersonic gas passing through a circular micro-channel under different inflow conditions

Guang-Ming Guo(郭广明), Qin Luo(罗琴), Lin Zhu(朱林), Yi-Xiang Bian(边义祥)
Chin. Phys. B, 2019, 28 (**6**): 064702. DOI: 10.1088/1674-1056/28/6/064702

A new kind of hairpin-like vortical structure induced by cross-interaction of sinuous streaks in turbulent channel

Jian Li(李健), Gang Dong(董刚), Hui Zhang(张辉), Zhengshou Chen(陈正寿), Zhaode Zhang(张兆德)
Chin. Phys. B, 2018, 27 (**8**): 084701. DOI: 10.1088/1674-1056/27/8/084701

Three-dimensional turbulent flow over cube-obstacles

Hao Lu(卢浩), Wen-Jun Zhao(赵文君), Hui-Qiang Zhang(张会强), Bing Wang(王兵), Xi-Lin Wang(王希麟)
Chin. Phys. B, 2017, 26 (**1**): 014703. DOI: 10.1088/1674-1056/26/1/014703

Hydromagnetic flow of a Cu–water nanofluid past a moving wedge with viscous dissipation

A. M. Salem, Galal Ismail, Rania Fathy
Chin. Phys. B, 2014, 23 (**4**): 044402. DOI: 10.1088/1674-1056/23/4/044402

Influences of Marangoni convection and variable magnetic field on hybrid nanofluid thin-film flow past a stretching surface

Noor Wali Khan[1], Arshad Khan[2,†], Muhammad Usman[1], Taza Gul[1,3], Abir Mouldi[4], and Ameni Brahmia[5]

[1] *Department of Mathematics, City University of Science and IT, Peshawar* 25000, *Pakistan*
[2] *College of Aeronautical Engineering, National University of Sciences and Technology (NUST), Sector H-12, Islamabad* 44000, *Pakistan*
[3] *Higher Education Archives and Libraries Department KP, Govt. Superior Science College, Peshawar, Pakistan*
[4] *Department of Industrial Engineering, College of Engineering, King Khalid University, Abha* 61421, *KSA*
[5] *Chemistry Department, College of Science, King Khalid University, Abha* 61413, *Saudi Arabia*

(Received 12 September 2021; revised manuscript received 23 October 2021; accepted manuscript online 17 November 2021)

Investigations on thin-film flow play a vital role in the field of optoelectronics and magnetic devices. Thin films are reasonably hard and thermally stable but quite fragile. The thermal stability of a thin film can be further improved by incorporating the effects of nanoparticles. In the current work, a stretchable surface is considered upon which hybrid nanofluid thin-film flow is taken into account. The idea of augmenting heat transmission by making use of a hybrid nanofluid is a focus of the current work. The flow is affected by variations in the viscous forces, along with viscous dissipation effects and Marangoni convection. A time-constrained magnetic field is applied in the normal direction to the flow system. The equations governing the flow system are shifted to a non-dimensional form by applying similarity variables. The homotopy analysis method is employed to find the solution to the resultant equations. It is noticed in this study that the flow characteristics decline with augmentation of magnetic, viscosity and unsteadiness parameters while they increase with enhanced values of thin-film parameters. Thermal characteristics are supported by increasing values of the Eckert number and the unsteadiness parameter and opposed by the viscosity parameter and Prandtl number. The numerical impact of different emerging parameters upon skin friction and the Nusselt number is calculated in tabular form. A comparison of current work with established results is carried out, with good agreement.

Keywords: thin-film flow, hybrid nanofluid, viscous dissipation, stretching surface, homotopy analysis method

PACS: 44.15.+a, 47.27.nd, 47.15.gm **DOI:** 10.1088/1674-1056/ac3a5d

1. Introduction

Recently thin-film flow has obtained considerable significance due to its important applications at the industrial level such as coating of fibers and cables, cooling of metallic plates, processing of foodstuffs, extrusion of plastic surface thinning and annealing of copper wires.[1] Researchers have been inspired by the pioneering work of Wang,[2] who investigated the time-dependent flow of a thin film over a stretchable surface. Wang's[2] ideas were further extended by Andersson *et al.*[3] to improve heat transmission characteristics. Afterwards, Liu and Andersson[4] presented the idea of thin-film flow in a more generalized form. Wang[5] performed an analytical solution using the homotopy analysis method (HAM) for thin-film flow upon a time-dependent stretched sheet. Wang compared the results of HAM with the numerical solution and found a good agreement between the results. Iqbal *et al.*[6] analyzed thin-film flow upon an unsteady surface using thermophoresis effects and Brownian motion. They observed that the thermal profiles were augmented by a corresponding increase in Brownian and thermophoresis parameters. Sadiq[7] analyzed the thermal characteristics for thin-film nanoparticles upon a stretched surface by using the temperature of the surface and an internal heat generation source. Sadiq used water as the base fluid with copper, titanium and alumina nanoparticles, and proved that augmentation of the volumetric fraction of solid nanoparticles reduced the flow and enhanced the thermal characteristics.

The suspension of small-sized particles (of a size $<$ 100 nm, i.e., nanoparticles) in a base fluid results in a nanofluid.[8,9] It has been proved experimentally[8] that nanofluids has higher thermal flow characteristics than traditional fluids. Additionally, hybrid nanofluids have attracted the attention of researchers due to their wide range of applications in the fields of medicine, nanotechnology and the phenomenon of thermal transmission. Khan *et al.*[10–12] published an excellent analysis of heat transmission by hybrid nanofluids using various flow conditions and different graphical views. They proved that the rate of thermal flow is much better for hybrid nanofluids compared with traditional fluids. Due to the use of hybrid nanofluids, as investigated by Hayat *et al.*,[13] applications in many fields such as biomedicines, conservation of energy, ceramics, optics and nanotechnology have been updated. Khan *et al.*[14] researched the thermal flow of a carbon nanotube nanofluid between two rotating plates. The authors of this investigation used various flow conditions and high-

†Corresponding author. E-mail: arshad8084@gmail.com
© 2022 Chinese Physical Society and IOP Publishing Ltd

lighted that thermal diffusivity of the fluid was augmented with enhancement in thermal radiation and Brownian motion. Pal and Mandal[15] discussed the flow of a hybrid nanofluid past a stretched surface with impact of a magnetic field. Xu *et al.*[16–19] carried out some impressive work to improve the flow and heat transfer of a nanofluid by using various flow conditions with different geometrical views. In these investigations the authors made an attempt to fill the gaps in the existing literature.

Viscous dissipation is caused by devastation of a fluctuating velocity gradient due to viscous stresses. This irreparable procedure normally leads to the conversion of kinetic energy to internal energy of the fluid and causes heating of the flow system. Pop[20] analyzed the idea of energy dissipation and transportation at the nanoscale and also highlighted that this concept is of great importance in designing energy conservation systems and energy-efficient circuits. Ali *et al.*[21] examined the impact of viscous dissipation upon thermal flow for hybrid nanoparticles in a porous channel. It was noticed in that study that the thermal profiles were augmented with the enhancement of energy dissipation. Sharma *et al.*[22] inspected the effects of forced convection heat transmission on time-dependent fluid flow between rotary discs. In that work the authors used the basic concept of the Neuringer–Rosensweig model for flow equations. They noted that the dissipation parameter caused an augmentation in thermal flow. Augusto *et al.*[23] employed the concept of thermal flow and viscous dissipation for the reduction of friction inside a grease-filled labyrinth seal. They used an Arrhenius-type equation in their mathematical modeling. Khan *et al.*[24–26] analyzed the augmentation of heat transfer and thermal flow by a thin moving needle surrounded by a moving fluid. In these investigations, the authors used the impact of viscous dissipation along with other flow conditions and established that thermal flow and heat transmission were augmented by enhancing the values of the viscous parameter.

The inspection of viscous fluid flow upon a stretching surface is of significant importance due to practical applications in numerous manufacturing procedures such as copper wire drawing, fabrication of glass, stretching of artificial fibers and plastic films, and polymer extrusions, etc. The performance of the final product depends upon the rate of mass and thermal flow over the stretching surface, as examined by Karwe and Jaluria.[27] Lund *et al.*[28] analyzed the Tiwari and Das model using the thermophoresis characteristics of nanoparticle fluid flow upon a porous stretching surface. In that study, the authors used copper and alumina nanoparticles in water as the base fluid. Abbas *et al.*[29] investigated the inclined stretching surface of the flow of a hybrid nanofluid using the Xue and Yamada–Ota models. Zainal *et al.*[30] highlighted the stability concept of a magnetohydrodynamic nanoparticle flow upon a stretching sheet with the squared velocity term. Anuar *et al.*[31] explored the effects of buoyancy on hybrid nanofluid flow over a stretching plate using silver and magnesium oxide nanoparticles. They noted that velocity declined while thermal flow was enhanced with increased volumetric fraction of nanoparticles. Readers can find more information about the related work in Refs. [32–41].

Several investigations have been conducted into thin-film flow over a stretching sheet by employing different flow conditions, but no work has yet been carried out on thin-film flow of a hybrid nanofluid with variable viscosity influenced by Marangoni convection, which is the main motivation for this work. In the current work, a stretchable surface is considered upon which flow of a hybrid nanofluid thin film is taken into account. The current work focuses on the idea of augmenting heat transmission by making use of a hybrid nanofluid. The equations that govern the flow problem will be converted to dimensionless form by employing a set of similar variables. The resultant set of equations will then be solved by using HAM.

2. Mathematical formulation

Consider an unsteady two-dimensional thin-film flow of a hybrid nanofluid upon a stretching surface affected by a magnetic field applied in the direction normal to the flow of fluid. The stretched velocity of the surface is $U_w = bx/1-at$, where b and γ are fixed values. To augment the heat transfer characteristics of the fluid flow, titanium oxide and silver nanoparticles were incorporated into the base fluid. The flow is also influenced by variable viscosity and Marangoni convection. The fixed concentration and temperature of the hybrid nanofluid are C_0 and T_0, respectively, whereas these respective quantities at the surface of the sheet are $C_w(x,t) = C_r(bx^2/2\nu)(1-at)^{-3/2}$ and $T_w(x,t) = T_0 - T_r(bx^2/2\nu)(1-at)^{-3/2}$ with C_r and T_r being the reference values of the nanofluid, such that $0 < C_r < C_0$ and $0 < T_r < T_0$.

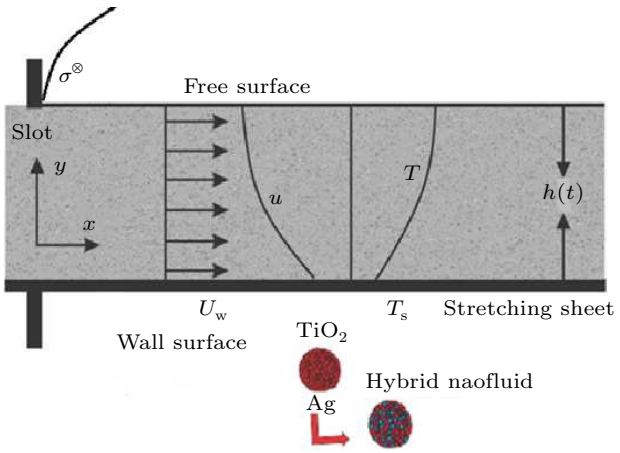


Fig. 1. Graphical view of the flow problem.

By implementing the above assumptions, the flow and thermal equations can be described as

$$\frac{\partial u}{\partial x}+\frac{\partial v}{\partial y}=0, \tag{1}$$

$$\rho_{\rm hnf}\left[\frac{\partial u}{\partial t}+u\frac{\partial u}{\partial x}+v\frac{\partial u}{\partial y}\right]=\frac{\partial}{\partial y}\left(\mu(T)_{\rm hnf}\frac{\partial u}{\partial y}\right)-\sigma^{*}B^{2}(t)u, \tag{2}$$

$$(\rho C_{\rm p})_{\rm hnf}\left[\frac{\partial T}{\partial t}+u\frac{\partial T}{\partial x}+v\frac{\partial T}{\partial y}\right]=k_{\rm hnf}\frac{\partial^{2}T}{\partial y^{2}}+\mu(T)_{\rm hnf}\left(\frac{\partial u}{\partial y}\right)^{2}. \tag{3}$$

The above equations are governed by the following physical conditions:

$$\begin{aligned}&u=U_{\rm w},\ v=0,\ T=T_{\rm w},\ \text{ at }\ y=0,\\&\mu_{\rm hnf}(T)\frac{\partial u}{\partial y}=\frac{\partial\sigma^{\otimes}}{\partial T}\frac{\partial T}{\partial x},\\&\frac{\partial T}{\partial y}=0\ \text{ and }\ v=u\frac{\partial h}{\partial t}\ \text{ at }\ y=h(t).\end{aligned} \tag{4}$$

In Eq. (4) the surface tension is denoted by $\sigma^{\otimes}=\sigma_0[1-\gamma(T-T_{\rm b})]$, with $\gamma=(\partial\sigma^{\otimes}/\partial T)_{T=T_0}$ having a fixed value. Moreover, the flow components along the coordinate axes are u and v, while the heat capacity, thermal conductivity and density of the hybrid nanoparticles are $(\rho C_{\rm p})_{\rm hnf}k_{\rm hnf}$ and $\rho_{\rm hnf}$, respectively.

2.1. The Reynolds model

In this model,

$$\mu(T)_{\rm hnf}=\frac{\mu_{\rm f}}{(1-\phi_1)^{2.5}(1-\phi_2)^{2.5}}{\rm e}^{-m(T-T_\infty)}, \tag{5}$$

where T_∞ is the temperature at the free stream and m is the variation exponent of viscosity.

The dimensionless variables are as follows:

$$\begin{aligned}&u=\frac{\partial\psi}{\partial y}\ \text{ and }\ v=-\frac{\partial\psi}{\partial y},\ \eta=\left(\frac{b}{\upsilon_{\rm f}(1-at)}\right)^{1/2}y,\\&\psi(x,y,t)=\left(\frac{\upsilon_{\rm f}b}{1-at}\right)^{1/2}xf(\eta),\\&\beta=\frac{b}{\upsilon_{\rm f}(1-at)^{1/2}}h(t),\\&T(x,y,t)=T_0-T_{\rm r}\left(bx^{2}/2\upsilon_{\rm f}\right)(1-at)^{-3/2}\Theta(\eta),\\&\Lambda=m(T_{\rm w}-T_\infty).\end{aligned} \tag{6}$$

By incorporating Eq. (6) into the system of modeled equations we have

$$f'''+\frac{\mu_{\rm f}}{\mu_{\rm hnf}}\frac{\rho_{\rm hnf}}{\rho_{\rm f}}{\rm e}^{\Lambda\Theta}\left[ff''-(f')^{2}-S(f'+\frac{\eta}{2})f''\right]-M\frac{\sigma_{\rm hnf}}{\sigma_{\rm f}}\frac{\mu_{\rm f}}{\mu_{\rm hnf}}f'=0, \tag{7}$$

$$\frac{k_{\rm hnf}}{k_{\rm f}}\Theta''+Pr\frac{(\rho C_{\rm p})_{\rm hnf}}{(\rho C_{\rm p})_{\rm f}}\left[f\Theta'-2f'\Theta-\frac{S}{2}(3\Theta+\eta\Theta')\right]+\frac{\mu_{\rm hnf}}{\mu_{\rm f}}{\rm e}^{-\Lambda\Theta}PrEc(f'')^{2}=0. \tag{8}$$

Some physical parameters are encountered while changing the governing system of equations to dimensionless form, which are defined mathematically as

$$\begin{aligned}&S=\frac{\gamma}{b},\ M=\frac{\sigma^{*}B_0^{2}}{\rho_{\rm f}b},\ Pr=\frac{\mu_{\rm f}C_{\rm p}}{k_{\rm f}},\\&Ec=\frac{U_{\rm w}^{2}}{C_{\rm p}(T_{\rm w}-T_0)},\ \Gamma=\frac{\gamma\sigma_0T_{\rm ref}}{\mu_{\rm f}\sqrt{b\upsilon_{\rm f}}}.\end{aligned} \tag{9}$$

Here S is unsteadiness parameter, M is a magnetic parameter, Pr is the Prandtl number, Ec is the Eckert number, Γ is the Marangoni convection parameter and Λ is the viscosity parameter.

The conditions at the boundaries in the dimensionless form are converted as

$$\begin{aligned}&f(0)=0,\ f(\beta)=\frac{S\beta}{2},\ f'(0)=1,\\&\frac{\mu(T)_{\rm hnf}}{\mu_{\rm f}}f''(\beta)=\Gamma\Theta(\beta),\ \Theta(0)=1,\ \Theta'(\beta)=0.\end{aligned} \tag{10}$$

The thermophoresis characteristics of traditional and hybrid nanofluids are shown in Table 1 while their numerical values are given in Table 2.

Table 1. Thermophysical characteristics of TiO_2 and (TiO_2 + Ag/blood) nanofluid.[42]

Properties	Nanofluid (TiO_2)	Hybrid nanofluid (TiO_2 + Ag/blood)
Density	$\rho_{\rm nf}=(1-\varphi_1)\rho_{\rm f}+\varphi_1\rho_{\rm s1}$	$\rho_{\rm hnf}=\left\{(1-\varphi_2)\left((1-\varphi_1)+\varphi_1\frac{\rho_{\rm s1}}{\rho_{\rm f}}\right)+\varphi_2\frac{\rho_{\rm s2}}{\rho_{\rm f}}\right\}\rho_{\rm f}$
Heat capacity	$(\rho C_{\rm p})_{\rm nf}=(1-\varphi_1)(\rho C_{\rm p})_{\rm f}+\varphi_1(\rho C_{\rm p})_{\rm s1}$	$(\rho C_{\rm p})_{\rm hnf}=\left\{(1-\varphi_2)\left((1-\varphi_1)+\varphi_1\frac{(\rho C_{\rm p})_{\rm s1}}{(\rho C_{\rm p})_{\rm f}}\right)+\varphi_2\frac{(\rho C_{\rm p})_{\rm s2}}{(\rho C_{\rm p})_{\rm f}}\right\}(\rho C_{\rm p})_{\rm f}$
Dynamic viscosity	$\mu_{\rm nf}=\frac{\mu_{\rm f}}{(1-\varphi_1)^{2.5}}$	$\mu_{\rm hnf}=\frac{\mu_{\rm f}}{(1-\varphi_1)^{2.5}(1-\varphi_2)^{2.5}}$
Thermal conductivity	$\kappa_{\rm nf}=\frac{\kappa_{\rm s1}+2\kappa_{\rm f}-2\varphi_1(\kappa_{\rm f}-\kappa_{\rm s1})}{\kappa_{\rm s1}+2\kappa_{\rm f}+\varphi_1(\kappa_{\rm f}-\kappa_{\rm s1})}\kappa_{\rm f}$	$\kappa_{\rm hnf}=\frac{\kappa_{\rm s2}+2\kappa_{\rm f}-2\varphi_2(\kappa_{\rm f}-\kappa_{\rm s2})}{\kappa_{\rm s2}+2\kappa_{\rm f}+\varphi_2(\kappa_{\rm f}-\kappa_{\rm s2})}\kappa_{\rm nf}$

Table 2. Numerical values of TiO_2 and $TiO_2 + Ag$/blood nanofluid for thermophysical properties.

Properties	TiO_2 nanoparticles	Ag nanoparticles	Pure blood base fluid
ρ (kg/m^3)	4250	10500	1063
C_p (J·kg^{-1}·K^{-1})	686.2	235	3594
κ (W/mK)	8.954	429	0.492

3. Solution method

It is a common observation that most physical phenomena when modeled mathematically give rise to a nonlinear equation. Sometimes, the resultant set of equations is highly nonlinear. To solve such models, researchers and mathematicians have designed certain tools and techniques. HAM[12,43,44] is one technique that is used to determine the semi-numerical solution to such problems. This method requires some starting values, which are defined below.

The operators π_f, π_Θ, and π_Φ in linear form are expressed as

$$\pi_f = \frac{\partial^4 f}{\partial \xi^4}, \quad \pi_\Theta = \frac{\partial^2 \Theta}{\partial \xi^2}. \tag{11}$$

The expanded form of these operators is

$$\pi_f(\chi_1 + \chi_2 \xi + \chi_3 \xi) = 0, \quad \pi_\Theta(\chi_4 + \chi_5 \xi) = 0. \tag{12}$$

The series expansion in Taylor's series form is given below:

$$f(\xi;\rho) = f_0(\xi) + \sum_{x=1}^{\infty} f_x(\xi)\rho^x, \tag{13}$$

$$\Theta(\xi;\rho) = f_0(\xi) + \sum_{x=1}^{\infty} \Theta_x(\xi)\rho^x. \tag{14}$$

Now

$$f_x(\xi) = \frac{1}{x}\frac{\mathrm{d}f(\xi;\rho)}{\mathrm{d}\xi}|_{\rho=0}, \quad \Theta_x(\xi) = \frac{1}{x}\frac{\mathrm{d}\Theta(\xi;\rho)}{\mathrm{d}\xi}|_{\rho=0}. \tag{15}$$

Further, we can write

$$L_f[f_x(\xi) - N_x f_{x-1}(\xi)] = \pi_f R_x^f(\xi), \tag{16}$$

$$L_\Theta[\Theta_x(\xi) - N_x \Theta_{x-1}(\xi)] = \pi_\Theta R_x^\Theta(\xi), \tag{17}$$

where $N_x = 0$ if $\rho \leq 1$ and $\rho > 1$.

4. Discussion of results

In the current work, a stretchable surface is considered upon which hybrid nanofluid thin-film flow is taken into account. In this work we consider the idea of augmentation of heat transmission by making use of a hybrid nanofluid. The flow is affected by variations in the viscous forces along with viscous dissipation effects and Marangoni convection. A time-constrained magnetic field is applied in the direction normal to the flow system. During the conversion of the equations that govern the flow system into dimensionless form, some physical parameters have been encountered. The effects of these parameters upon flow profiles are now discussed in detail with the help of a graphical view, as given below.

4.1. Flow characteristics

The impact of variations in different emerging parameters upon flow profiles is depicted in Figs. 2–5.

Figure 2 shows that change in the magnetic parameter M reduces the flow profiles. Physically this can be interpreted as follows: with increasing value of M a Lorentz force is produced that acts in the opposite direction to the flow of fluid and causes resistance to the fluid's motion. Due to these resistive effects the fluid flow declines.

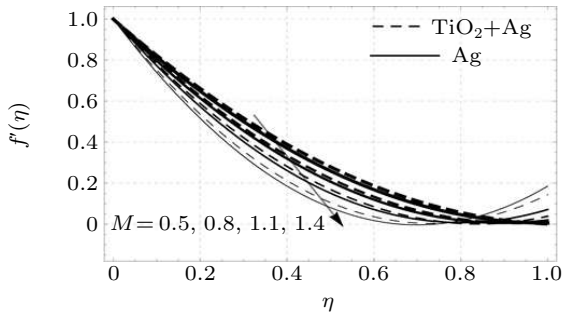


Fig. 2. Flow profiles versus magnetic parameter.

Figure 3 shows that an increase in the value of the viscosity parameter Λ results in a reduction of the velocity profiles. Actually, with an increase in the value of Λ the viscous forces increase, and as a result more resistance is experienced by the nanoparticles during motion. In this physical phenomenon, the thickness of the momentum boundary layer is reduced, causing the velocity profiles to decline.

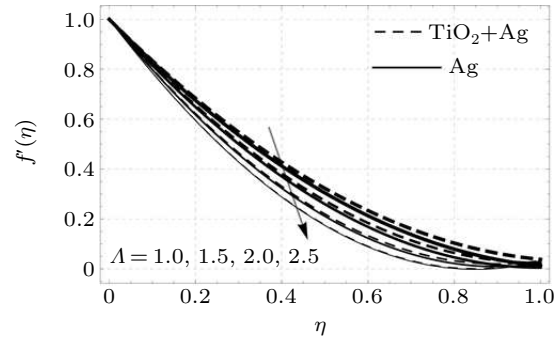


Fig. 3. Flow profiles versus viscosity parameter.

From Fig. 4 we can see that velocity is reduced in response to an increase in the unsteadiness parameter S. Physically this can be interpreted as follows: an increase in the value of S causes more resistive force to the fluid motion and increases the skin friction. In this whole process, the strength of the momentum layer is reduced, ultimately decreasing the velocity of the nanoparticles.

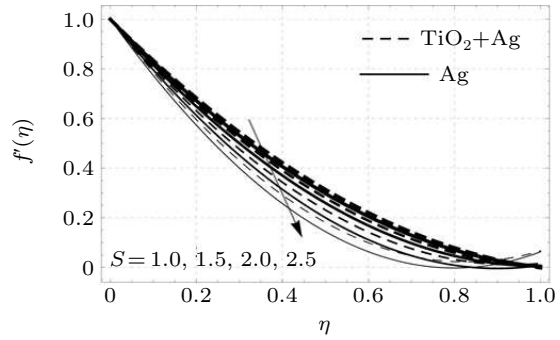


Fig. 4. Flow profiles versus unsteadiness parameter.

Figure 5 shows the impact of the thin-film parameter β upon the flow of fluid. An increase in the value of β leads to strengthening of the thickness of the momentum boundary layer, as a result of which the flow characteristics of the fluid increase.

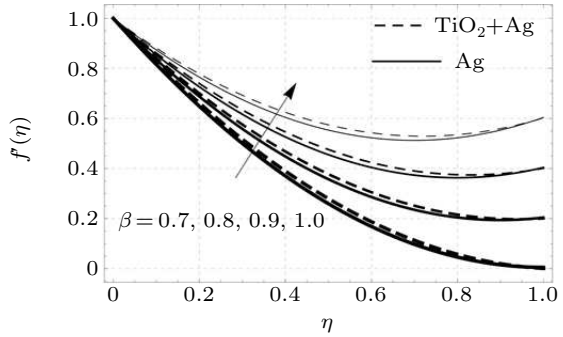


Fig. 5. Flow profiles versus thin film parameter.

4.2. Thermal characteristics

The impact upon flow profiles in response to variations in different emerging parameters has depicted in Figs. 6–9.

A change in thermal profiles in response to variations in the Eckert number Ec is presented in Fig. 6. It can be observed that with a growth in the value of Ec the transmission of energy increases from higher to lower regions. In this process kinetic energy changes to heat energy, leading to growth in the thermal profiles.

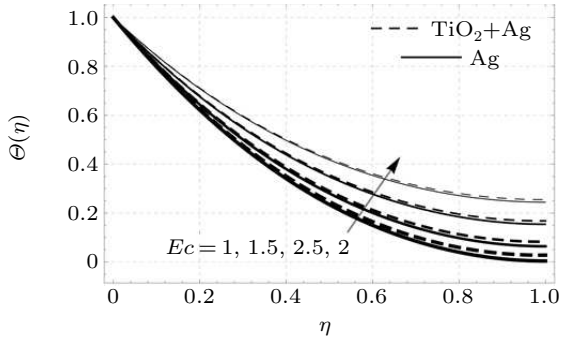


Fig. 6. Thermal profiles versus Eckert number.

Figure 7 depicts that the thermal characteristics decline with augmentation in Prandtl number Pr. Actually, at lower values of Pr more heat diffuses while at higher values of Pr less heat diffuses. Hence an increase in the value of Pr causes a reduction in thermal diffusion, leading to a decline in thermal characteristics.

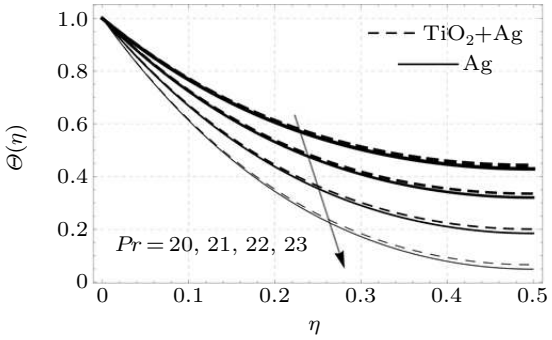


Fig. 7. Thermal profiles versus Prandtl number.

Figure 8 depicts that for increasing values of the unsteadiness parameter S more heat transfer occurs from regions of higher concentration to lower ones. This phenomenon strengthens the thickness of the thermal layer and causes an enhancement in the heat transfer.

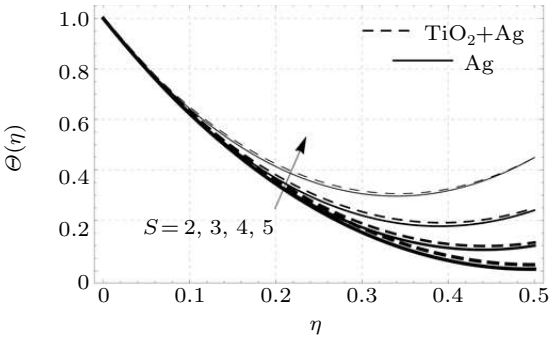


Fig. 8. Thermal profiles versus unsteadiness parameter.

Figure 9 portrays the influence of variations in the viscosity parameter Λ upon heat transmission. It can be noticed from this figure that for increasing values of Λ the thickness of the thermal layer decreases, as a result of which there is less heat diffusion. In this physical process, heat transmission declines as depicted in Fig. 9.

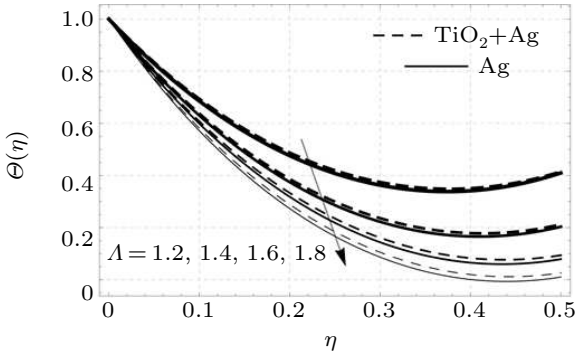


Fig. 9. Thermal profiles versus viscosity parameter.

4.3. Discussion of the tables

The thermophysical properties of nanoparticles are presented in Table 1 while their numerical values are depicted

in Table 2. The impact of various parameters on the thermal transfer rates for hybrid and traditional nanofluids is described numerically in Table 3. It can be seen that the Nusselt number increases with higher values of Ec, volumetric fraction of solid nanoparticles and the thin-film parameter while it declines with growth in the value of the viscosity parameter. The rate of heat transmission for hybrid nanoparticles has been noted to be much better than of a traditional nanofluid. A comparative analysis of current results and those published in the literature by Qasim *et al.*[45] was also carried out in the current investigation with regard to variations in common parameters. This comparison is presented in Table 4, where good agreement is noticed. In Fig. 10 the percentage augmentation in the rate of thermal flow is presented with a comparison between TiO_2 nanoparticles and $(TiO_2 + Ag)$ nanoparticles. From this chart, it is quite obvious that the rate of thermal flow varies from 3.77% to 9.02% when the values for TiO_2 nanoparticles range from 0.01 to 0.03 whereas for the same range for $(TiO_2 + Ag)$ nanoparticles the thermal flow rate varies from 4.05% to 9.58%. This justifies that hybrid nanoparticles ensure a greater heat flow rate than traditional nanofluids.

Table 3. Comparison of the heat transfer rate of nanofluids and hybrid nanofluids.

Λ	β	Ec	ϕ_1	ϕ_2	$-\left(\frac{k_{nf}}{k_f}\right)\Theta'(0)$ for nanofluid	$-\left(\frac{k_{hnf}}{k_f}\right)\Theta'(0)$ for hybrid nanofluid
0.3	0.5	0.5	0.01	0.01	0.356412	0.0.355283
0.5			0.01		0.354210	0.3531312
0.7			0.02		0.3521023	0.35132621
	0.6				0.3553121	0.35223012
	0.7				0.35437521	0.35100213
		1			0.78632104	0.79578213
		1.5			0.98876210	1.08932943
			0.02	0.02	0.99742187	1.13201342
			0.03	0.03	1.203421642	1.41032145

Table 4. Comparison of the values of the common parameters in the current work and the work of Qasim *et al.*[45]

Ec	β	$f''(0)$ ([45])	$f''(0)$ (present work)	$-\Theta'(0)$ ([45])	$-\Theta'(0)$ (present work)
2	0.5	0.32532103	0.325312421	1.4342164	1.43420013
3		0.3252210	0.32521203	2.21356421	2.21353108
4		0.32510213	0.32509213	3.02175431	3.021723142
	0.6	0.34568521	0.345675421	1.23142310	1.231421212
	0.7	0.36574218	0.365731021	1.02146321	1.021462142

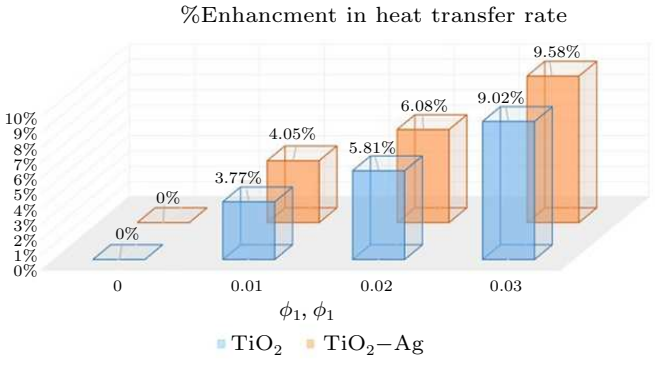


Chart. Percentage increase in heat transfer rate and comparison between nanofluids and hybrid nanofluids.

5. Conclusion

In this investigation, a stretchable surface is considered upon which a hybrid nanofluid thin-film flow is taken into account. In this work we focus on the idea of augmenting heat transmission by making use of a hybrid nanofluid. The flow is affected by variations in the viscous forces along with viscous dissipation effects and Marangoni convection. A time-constrained magnetic field is applied in the direction normal to the flow system. During the conversion of the equations that govern the flow system into dimensionless form, some physical parameters are encountered. The effects of these parameters on the flow profiles have been discussed in detail with the help of graphs. After a detailed discussion of the work the following points can be noted:

- When increasing the values of the magnetic parameter a Lorentz force is produced that acts in the opposite direction to the fluid flow and causes resistance to fluid motion. Due to these resistive effects the fluid flow declines.
- As the values of the viscosity parameter increase the viscous forces increases, due to which more resistance is experienced by the nanoparticles during the motion that in turn weakens the velocity profile. The same effects were noticed for increase in the unsteadiness parameter with fluid motion.
- Increase in the thin film parameter leads to strengthening of the thickness of the momentum boundary layer,

as a result of which the flow characteristics of the fluid improve.

- The transfer of energy increases with increase in the value of the Eckert number, which leads to growth of the thermal profile.
- Increase in the Prandtl number results in a reduction in thermal diffusion that causes a decline in thermal characteristics.
- With increase in the value of the unsteadiness parameter more heat transfer takes place from regions of higher concentration to regions of lower concentration, due to which an enhancement in heat transfer occurs.
- With increasing value of the viscosity parameter, the thickness of the thermal layer is reduced; as a result less heat diffuses and ultimately heat transmission declines.
- It is also established that the rate of thermal flow varies from 3.77% to 9.02% when the values of TiO_2 nanoparticles range from 0.01 to 0.03 whereas for the same range of values of $(TiO_2 + Ag)$ nanoparticles the thermal flow rate varies from 4.05% to 9.58% demonstrating that hybrid nanoparticles ensure a greater heat flow rate than a traditional nanofluid.

Acknowledgment

We thank the Deanship of Scientific Research at King Khalid University for funding this work through research groups (Grant No. RGP.1/260/42).

Appendix A

Table A1. Nomenclature.

u, v	Velocity components ($m \cdot s^{-1}$)	M	Magnetic parameter
B_0	Magnetic field strength ($N \cdot m \cdot A^{-1}$)	Pr	Prandtl number
T_0	Surface temperature (K)	Ec	Eckert number
T	Free surface temperature (K)	C_p	Specific heat capacity ($J \cdot kg^{-1} \cdot K^{-1}$)
f'	Dimensionless velocity	Γ	Marangoni convection parameter
k	Thermal conductivity ($W \cdot m^{-1} \cdot K^{-1}$)	S	Unsteadiness parameter
Λ	Viscosity parameter		
Greek symbols			
μ	Dynamic viscosity (mPa)	ρ	Density ($kg \cdot m^{-3}$)
η	Similarity variable	σ	Electrical conductivity
Θ	Dimensionless temperature	β	Thin film parameter
Subscripts			
hnf	Hybrid nanofluid	nf	Nanofluid
f	Base fluid		

References

[1] Aziz R C, Hashim I and Alomari A K 2011 *Meccanica* **46** 349
[2] Wang C Y 1990 *Quarterly of Applied Mathematics* **48** 601
[3] Andersson H I, Aarseth J B and Dandapat B S 2000 *International Journal of Heat and Mass Transfer* **43** 69
[4] Liu I C and Andersson H I 2008 *International Journal of Thermal Sciences* **47** 766
[5] Wang C 2006 *Heat and Mass Transfer* **42** 759
[6] Iqbal K, Ahmed J, Khan M, Ahmad L and Alghamdi M 2020 *Applied Physics A* **126** 1
[7] Sadiq M A 2021 *Journal of Thermal Analysis and Calorimetry* **143** 2075
[8] Choi S U S and Eastman J A 1995 *Enhancing thermal conductivity of fluids with nanoparticles*, No ANL/MSD/CP-84938; CONF-951135-29 Argonne National Lab, IL United States
[9] Choi S U S 2009 *Journal of Heat Transfer* **131**
[10] Jawad M, Khan A and Shah S A A 2021 *Brazilian Journal of Physics* **51** 1096
[11] Khan A, Shah Z, Alzahrani E and Islam S 2020 *International Communications in Heat and Mass Transfer* **119** 104979
[12] Islam S, Khan A, Kumam P, Alrabaiah H, Shah Z, Khan W, Zubair M and Jawad M 2020 *Scientific Reports* **10** 1
[13] Hayat T, Kiran A, Imtiaz M and Alsaedi A 2017 *Results in Physics* **7** 823
[14] Khan A, Shah Z, Islam S, Dawar A, Bonyah E, Ullah H and Khan A 2018 *AIP Advances* **8** 125024
[15] Pal D and Mandal G 2021 *International Journal of Ambient Energy* 1
[16] Xu H, Xing Z and Vafai K 2019 *International Journal of Heat and Fluid Flow* **77** 242
[17] Xu H J, Xing Z B, Wang F Q and Cheng Z M 2019 *Chemical Engineering Science* **195** 462
[18] Xu H and Xing Z 2017 *International Communications in Heat and Mass Transfer* **89** 73
[19] Xu H J, Liang G, Huang S B and Xu M H 2015 *International Journal of Heat and Mass Transfer* **83** 399
[20] Pop E 2010 *Nano Research* **3** 147
[21] Ali A, Noreen A, Saleem S, Aljohani A F and Awais M 2021 *Journal of Thermal Analysis and Calorimetry* **143** 2367
[22] Sharma K, Vijay N, Makinde O D, Bhardwaj S B, Singh R M and Mabood F 2021 *Chaos, Solitons and Fractals* **148** 111055
[23] Augusto L L X, Takahama M H, Negrão C O R and Cousseau T 2021 *Tribology International* **153** 106571
[24] Khan A, Saeed A, Tassaddiq A, Gul T, Mukhtar S, Kumam P, Ishtiaq A and Kumam W 2021 *Case Studies in Thermal Engineering* 25 100989
[25] Khan A, Saeed A, Tassaddiq A, Gul T, Kumam P, Ali I and Kumam W 2021 *Scientific Reports* **11** 1
[26] Khan A, Kumam W, Khan I, Saeed A, Gul T, Kumam P and Ali I 2021 *Plos One* **16** e0249264
[27] Karwe M V and Jaluria Y 1991 *J. Heat Transfer* **113** 612
[28] Lund L A, Omar Z and Khan I 2021 *International Journal of Numerical Methods for Heat and Fluid Flow* **31** 3621
[29] Abbas N, Nadeem S, Saleem A, Malik M Y, Issakhov A and Alharbi F M 2021 *Chinese Journal of Physics* **69** 109
[30] Zainal N A, Nazar R, Naganthran K and Pop I 2021 *Alexandria Engineering Journal* **60** 915

[31] Anuar N S, Bachok N and Pop I 2021 *International Communications in Heat and Mass Transfer* **123** 105236
[32] Hussain A, Mohyud-Din S T and Cheema T A 2012 *Chin. Phys. Lett.* **29** 114705
[33] Luo X P and Cui F Z 2008 *Chin. Phys. Lett.* **25** 2111
[34] Lin Z P, Xu S Z and Bao Y 2020 *Acta Phys. Sin.* **69** 014401 (in Chinese)
[35] Ning L Z, Hu B, Ning B B and Tian W L 2016 *Acta Phys. Sin.* **65** 214401 (in Chinese)
[36] Ning L, Na Wang N and Yuan Z 2014 *Acta Phys. Sin.* **63** 104401 (in Chinese)
[37] Zhao M, Tang X, Huo W, Han L, Deng Z, Jiang Y and Jia H 2020 *Chin. Phys. B* **29** 048104
[38] Salem A M, Ismail G and Fathy R 2014 *Chin. Phys. B* **23** 044402
[39] Mukhopadhyay S, Arif M G and Pk M W A 2013 *Chin. Phys. B* **22** 124701
[40] Mukhopadhyay S, Bhattacharyya K and Hayat T 2013 *Chin. Phys. B* **22** 114701
[41] Mukhopadhyay S 2013 *Chin. Phys. B* **22** 114702
[42] Waini I, Ishak A and Pop I 2020 *Alexandria Engineering Journal* **59** 91
[43] Liao S J 1999 *International Journal of Non-Linear Mechanics* **34** 759
[44] Liao S J 2010 *Commun. Nonlinear Sci. Numer. Simul.* **15** 2003
[45] Qasim M, Khan Z H, Lopez R J and Khan W A 2016 *Euro. Phys. J. Plus* **131** 1